Available online at www.sciencedirect.com
ScienceDirect
Journal of Nuclear Materials 367–370 (2007) 257–262
journal of nuclear materials
www.elsevier.com/locate/jnucmat

Systematic group-specific trends for point defects in bcc transition metals: An ab initio study

D. Nguyen-Manh [a,*], S.L. Dudarev [a], A.P. Horsfield [b]

[a] EURATOM/UKAEA Fusion Association, Culham Science Centre, Abingdon, Oxfordshire OX14 3DB, UK
[b] Department of Physics and Astronomy, University College of London, London WC1E 6BT, UK

Abstract

Density functional theory calculations have been performed to study the systematic trends of point defect behaviours in bcc transition metals. We found that in all non-magnetic bcc transition metals, the most stable self-interstitial atom (SIAs) defect configuration has the $\langle 1\,1\,1\rangle$ symmetry. The calculated formation energy differences between the $\langle 1\,1\,0\rangle$ dumbbell and the lowest-energy $\langle 1\,1\,1\rangle$ configuration of metals in group 5B (V, Nb, Ta) are consistently larger than those of the corresponding element in group 6B (Cr, Mo, W). The predicted trends of SIA defects are fundamentally different from those in ferromagnetic α-Fe and correlate very well with the pronounced group-specific variation of thermally activated migration of SIAs under irradiation depending on the position of bcc metals in the periodic table.

1. Introduction

Body-centered cubic (bcc) transition metals and their alloys including a wide range of ferritic/martensitic steels were recently identified as prime candidate materials for fusion power plants with promising high strength and fracture toughness as well as appropriate radiation resistance [1]. Bcc-W is also a favoured material for plasma-facing surfaces in fusion power plants, mainly because of its high melting point and resistance to sputtering by low-energy light ions. It is, therefore, important to understand the fundamental materials science behaviour of these metals and alloys in a severe operating environment under intense fluxes of high-energy neutrons that can have a drastic influence on the life time of fusion power plants components. Among the non-equilibrium atomic defects in metals produced under irradiation, the interstitials are remarkable due to the large lattice perturbations they cause. Unlike vacancies which both form spontaneously and by displacements, the SIA defects are only generated in high-energy collision cascades. Both defect species may cluster or migrate to sinks which gives rise to swelling, irradiation creep and radiation embrittlement.

In bcc transition metals, interatomic bonds at the centre of an interstitial defect are strongly compressed and the directionality of d–d interactions is expected to play a more significant part in the core of the defect than in the less distorted regions

* Corresponding author. Tel.: +44 1235 466284; fax: +44 1235 466435.
E-mail address: duc.nguyen@ukaea.org.uk (D. Nguyen-Manh).

0022-3115/$ - see front matter © 2007 Elsevier B.V. All rights reserved.
doi:10.1016/j.jnucmat.2007.03.006

of the material [2]. The collected experimental defect data for bcc transition metals [3] show pronounced group-specific trends depending on the electron-to-atom ratio. In addition to the self-diffusion anomaly of the bcc high-temperature phases of group 4B (Ti, Zr and Hf), the enthalpies of formation [4] together with the thermally activated motion of screw dislocations [5] (having line and Burgers' vector along $\langle 1\,1\,1\rangle$) can be correlated with elastic properties for the bcc elements of groups 5B and 6B. While the formation and thermal migration energies of vacancies in metals can be measured experimentally, the formation energies of SIA defects are less accessible to direct observation due to the large displacements associated with interstials atoms. So far, the only systematic data on thermally activated migration of SIAs have been obtained from resistivity recovery experiments following electron irradiation. For group 5B metals (V, Nb, Ta), the resistivity recovery curves indicate that SIAs are mobile at very low temperature, about 6 K according to Ref. [3]. For other bcc transition metals, the long-range migration of SIAs defects start at 27 K in W, 35 K in Mo, 40 K in Cr and 120 K in magnetic α-Fe [6]. So far it has been difficult to formulate a consistent model explaining these trends. The main purpose of this paper is to show that these problems can be solved by performing a systematic study of all SIA configurations bcc transition metals using first-principles electronic structure based calculations.

2. Computational techniques

The present calculations have been performed within the density functional theory (DFT) as it has been implemented in the Package of Linear combination of Atomic Type Orbitals (PLATO) code using atomic-like basis sets [7] and in the Vienna ab initio Simulation Package (VASP) code using plane-wave basis sets [8]. More information about technical details of these calculations can be found in [9]. In both techniques, the Perdew–Burke–Ernzerhof (PBE) generalized gradient approximation (GGA) is used for exchange and correlation functional with semi-core electrons included within the pseudopotentials. It is important to emphasize that the inclusion of semi-core electrons in the valence states has a significant effect on predicting the formation energies of SIAs defects between the competing SIAs configurations for all the bcc metals considered. In particular, we found that the most stable $\langle 1\,1\,1\rangle$ configuration of SIAs cannot be reproduced correctly by ignoring them for transition metals in group 6B (Cr, Mo, W). There is overall agreement between PLATO and VASP predictions of defect formation energies and trends of different SIAs configurations. For example, in bcc-Ta we found the SIAs formation energies of 5.858, 5.859, 6.557, 6.845, 6.987 and 7.020 eV for the $\langle 1\,1\,1\rangle$ dumbbell, $\langle 1\,1\,1\rangle$ crowdion, $\langle 1\,1\,0\rangle$ dumbbell, tetrahedral, $\langle 1\,0\,0\rangle$ dumbbell and octahedral configurations from the VASP calculations, respectively, that are consistent with the PLATO results presented in Table 1. Unless stated otherwise, all results for SIA defects presented in this paper were obtained from the PLATO method using 129 atom cells. In case of Cr, calculations have been performed in the non-magnetic state where the cohesive energy is very close to those of anti-ferromagnetic configuration [9].

Table 1
Formation and migration enthalpies of mono-vacancy and formation energies of self-interstitial atom defects calculated for all bcc transition metals of group 5B (V, Nb, Ta) and 6B (Cr, Mo, W)

(eV)	V	Nb	Ta	Cr	Mo	W
H_{vac}	2.51	2.99	3.14	2.64	2.96	3.56
H_{mig}(vac)	0.62	0.90	1.48	0.91	1.28	1.78
$H_I\langle 1\,1\,1\rangle$	3.367	5.253	5.832	5.685	7.417	9.548
H_I crow.	3.371	5.254	5.836	5.660	7.419	9.551
$H_I\langle 1\,1\,0\rangle$	3.652	5.597	6.382	5.674	7.581	9.844
H_I tetra.	3.835	5.758	6.771	6.189	8.401	11.05
$H_I\langle 1\,0\,0\rangle$	3.918	5.949	7.003	6.643	9.004	11.49
H_I octa.	3.964	6.060	7.095	6.723	9.067	11.68

3. Results and discussion

3.1. Mono-vacancy formation and migration energies

Benchmark calculations of bulk properties in all bcc transition metals in group 5B and 6B have been presented in [9] and compare well with available experimental data. The vacancy calculations were also performed on $4\times4\times4$ super-cells with 127 atoms using both ionic and volume relaxations. The vacancy migration energies have been obtained by the nudged elastic band technique [10] for finding saddle points and minimum energy paths between known reactants and products with values shown in Fig. 1. The calculated enthalpies of formation and the migration energies of mono-vacancy in all bcc metals of group 5B and 6B are given in the first two rows of Table 1. To our best knowledge, these values of migration energies are reported systemati-

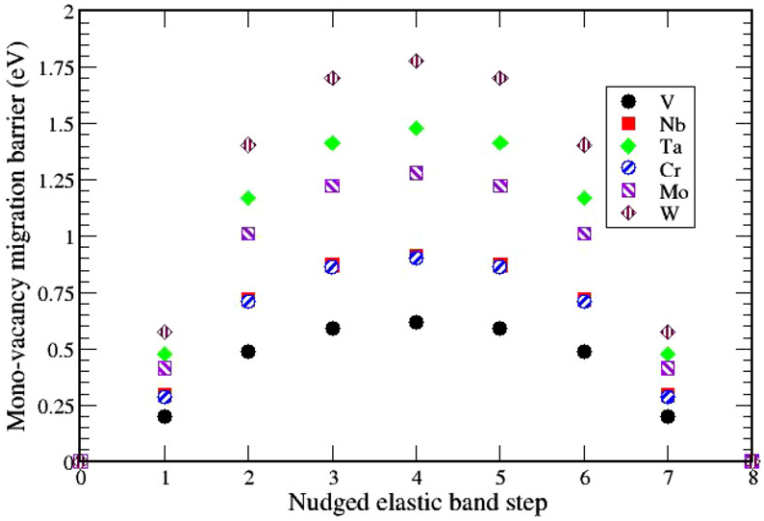

Fig. 1. Mono-vacancy energy barriers calculated for all bcc transition metals of group 5B (V, Nb, Ta) and 6B (Cr, Mo, W).

cally for the first time. Comparing with previous DFT calculations [11,12], we find that our calculations show better overall agreement with available experimental data [3,9]. In particular, experimental values for the vacancy migration energy in Mo have been reported by several groups. A rather reliable measurement from the group in Delft using helium desorption to measure vacancy concentration gave 1.23 ± 0.05 eV [13]. This value can be compared with the results of Yamakawa et al. of 1.30 ± 0.02 eV [14]. A combination of these two results suggests that the value of 1.28 eV predicted in this paper for vacancy migration energy in Mo is in an excellent agreement with available experimental measurements. Around the vacancy, we also find the inward relaxation of the first-nearest neighbour (NN) shell is of order 4% for all three metals in group 5B whereas for metals in group 6B it is reduced to about 1.2%. More importantly, both formation and migration enthalpy of mono-vacancies show a pronounced group-specific variation with a strong tendency for group 6B metals to have higher energies than the corresponding elements in group 5B.

3.2. Systematic trends of SIA defect energies

Fig. 2 shows the relaxed atomic structure and electron charge densities for the four SIA configurations: $\langle 1\,1\,1\rangle$ crowdion, $\langle 1\,1\,1\rangle$, $\langle 1\,1\,0\rangle$ and $\langle 1\,0\,0\rangle$ dumbbells in bcc-W. The darker colour highlights atoms situated in the highly deformed core region of defects with compressed bond lengths. The $\langle 1\,1\,1\rangle$ dumbbell configuration (two atoms sharing one lattice site) is found to be very similar to those of the crowdion one (four atoms sharing three lattice sites). In both configurations, the deformation is mainly confined to a single string along the [1 1 1] direction. The $\langle 1\,1\,0\rangle$ dumbbell configuration is closely related to the $\langle 1\,1\,1\rangle$ because its pattern of deformation can be considered as the formation of two superimposed $\langle 1\,1\,1\rangle$ type SIAs configuration on the (1 1 0) plane. Table 1 includes the calculated formation energies for all bcc metals of groups 5B and 6B. We found that the $\langle 1\,1\,1\rangle$ (dumbbell or crowdion) configuration has the lowest formation energies in all non-magnetic bcc transition metals followed by the $\langle 1\,1\,0\rangle$ configuration with the energy difference that is again consistently smaller in metals of group 6B than the corresponding ones in group 5B. These predictions confirm earlier DFT studies in bcc-V and bcc-Mo [15] but are fundamentally different from magnetic bcc Fe where the $\langle 1\,1\,0\rangle$ is found to be the most stable configuration in both DFT calculations [16,17] and the tight-binding bond Stoner model [18]. Our findings are at variance with defect energies predicted from the existing empirical many-body central-forces interatomic potentials [19] for which the $\langle 1\,1\,0\rangle$ dumbbell is the lowest-energy configuration. An exception to the rule is for bcc-W where the $\langle 1\,1\,1\rangle$ dumbbell configuration is found to be the most stable and is separated by an energy gap from the $\langle 1\,1\,0\rangle$ dumbbell of 0.75 eV. The latter is again however in disagreement with our ab initio prediction of 0.29 eV.

The group-specific trends in the SIAs formation energies relative to the $\langle 1\,1\,1\rangle$ configuration for all bcc metals of groups 5B and 6B is shown in Fig. 3

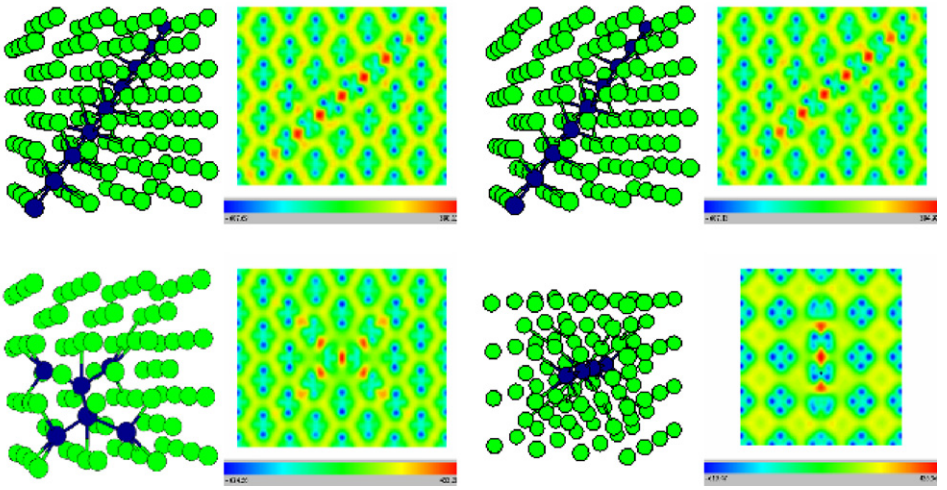

Fig. 2. Relaxed atomic configurations for SIA defects in bcc-W: ⟨1 1 1⟩ dumbbell (upper left-hand panel), ⟨1 1 1⟩ crowdion (upper right-hand panel), ⟨1 1 0⟩ dumbbell (lower left-hand panel), ⟨1 0 0⟩ dumbbell and the corresponding electronic charge density differences between the final and the atomic densities.

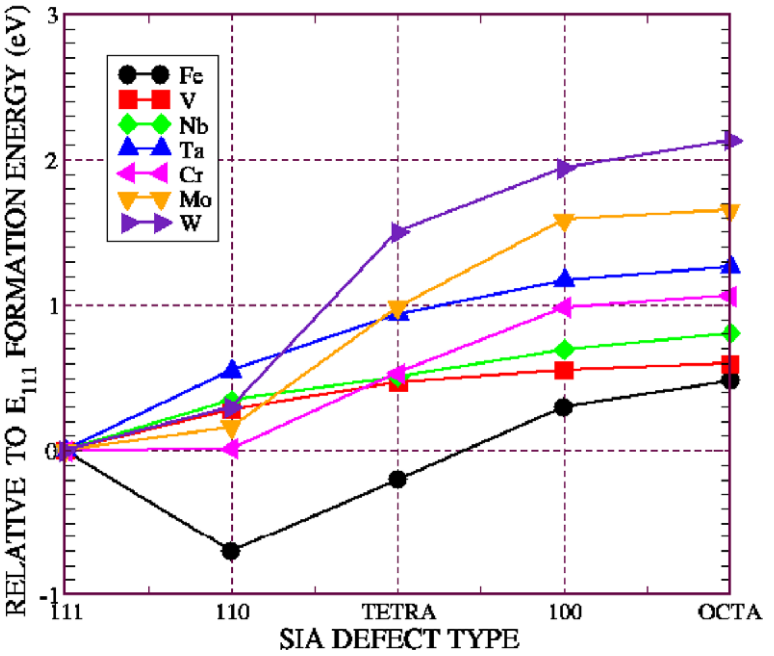

Fig. 3. Relative formation energies of several SIA configurations for all bcc transition metals with respect to the ⟨1 1 1⟩ configuration. Data for bcc-Fe is taken from Ref. [17].

and compared with those of ferromagnetic bcc Fe [17]. We see a striking dissimilarity in the pattern of ordering of SIAs defect energies between the non-magnetic bcc transition metals and bcc-Fe. The importance of the magnetic contribution to the formation energies of SIAs defects are discussed in [16–18], where the lowest-energy and immobile ⟨1 1 0⟩ dumbbell configuration owes its stability to magnetic ordering with an energy gap of 0.7 eV relative to the ⟨1 1 1⟩ configuration. The most notable trend is exhibited by the difference between the energies of the ⟨1 1 0⟩ and ⟨1 1 1⟩ configurations. This energy difference varies from 0.29 eV for V to 0.34 for Nb and to 0.55 eV for Ta compared with 0.01

for Cr, 0.16 for Mo and 0.29 for W showing the pronounced variation with position of materials in the periodic table of elements. Finally, we note from Fig. 2 that apart from the difference between energies of the ⟨1 1 0⟩ and ⟨1 1 1⟩ dumbbells, the other SIA configurations in bcc-Fe follow the same relative pattern as SIA configurations in groups 5B and 6B.

3.3. SIA migration mechanism

The larger energy differences between the ⟨1 1 0⟩ and ⟨1 1 1⟩ dumbbells make tantalum and tungsten good representative cases of group 5B and 6B, respectively, for studying the total-energy pathways between the ⟨1 1 1⟩, ⟨1 1 0⟩ and ⟨1 0 0⟩ defect configurations. While the energy pathways linking the ⟨1 1 1⟩ and ⟨1 0 0⟩ configurations in the two metals exhibit a similar behaviour [9], it is striking to find a quantitative difference between Ta and W in the shape of energy barriers describing the ⟨1 1 1⟩ to ⟨1 1 0⟩ transition shown in Fig. 4. We see that in tungsten the ⟨1 1 1⟩ SIAs configuration is characterized by the presence of a fairly soft bending mode transforming it into a ⟨1 1 0⟩ dumbbell whereas in tantalum the ⟨1 1 1⟩ defect is rigid and stable with respect to the same transition. Since there are three bending modes corresponding to each of the three (1 1 0) planes intersecting along the {1 1 1} directions, they can be easily excited even at low temperatures and give rise to high statistical weigh of the planer ⟨1 1 0⟩-like defect configurations observed in the X-ray diffuse scattering experiment for bcc-Mo [20]. It is important to emphasise here that due to the smaller energy difference between the ⟨1 1 1⟩ and ⟨1 1 0⟩ SIAs in bcc-Mo and bcc-Cr in comparison with bcc-W, the existence of these bending modes should have an increasingly stronger effect on the mobility of defect in the former two elements in group 6B. This observation agrees with the trend exhibited by increasing temperature in the stage I of recovery curves from 27 K in W to 40 K in Cr. Therefore, we should expect that while in groups 5B metals, the ⟨1 1 1⟩ SIA configuration performs one-dimensional motion in the [1 1 1] direction according to the Frenkel–Kontorova model [9,21,22], the mobility of SIA defect in group 6B is affected by the soft bending modes impeding thermally activated one-dimensional migration.

4. Conclusions

We have performed the first systematic first-principles studies of formation energy of different SIA configurations in bcc transition metals in group 5B and 6B. We have found that the calculated SIAs formation energies show very strong group-specific trends depending on the electron-to-atom ratio of materials in the periodic table. The ⟨1 1 1⟩ defect is found to be the lowest-energy SIA configuration in all non-magnetic bcc transition elements in striking contrast with the ⟨1 1 0⟩ configuration for bcc iron that is explained mainly by magnetism. We have shown that the energy difference between the

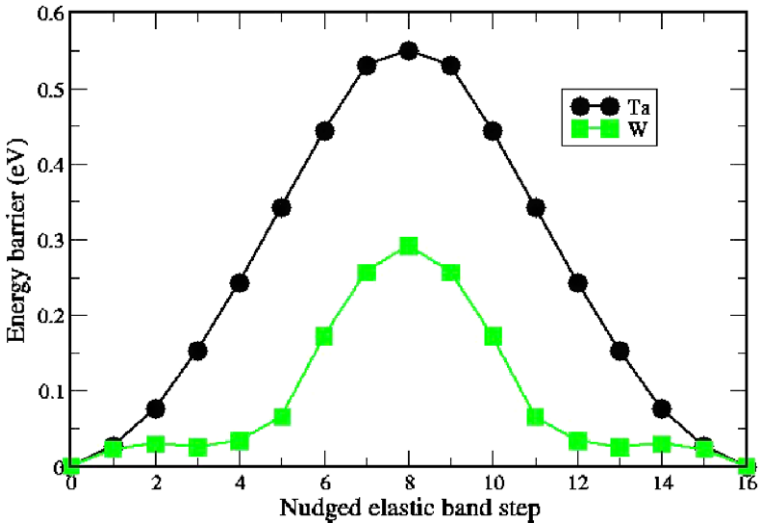

Fig. 4. Total-energy pathways between the ⟨1 1 1⟩ and ⟨1 1 0⟩ dumbbell configurations for bcc-W (group 6B) compared with those of bcc-Ta (group 5B).

$\langle 1\,1\,1\rangle$ and $\langle 1\,1\,0\rangle$ configurations is the main factor to differentiate the migration mechanism between group 5B and 6B, leading to group-specific behaviour of the onset of long-range migration observed in recovery experiments. Together with calculated formation and migration enthalpies for mono-vacancies, we conclude that the group-specific behaviour of defects in bcc transition metals has a pronounced relation to the electronic structure of materials, in particular with directional bonding contribution. This has an important implication in modelling of materials for fusion power plants.

Acknowledgements

We thank Ian Cook for encouragement and stimulating discussions. DNM would like to thank J. Evans for providing information on experimental values of vacancy migration energy in Mo. This work is funded by Integrated EXTREMAT Project, EURATOM and the United Kingdom EPSRC. We are grateful to T. Martin and P. Knight for their helps in using parallel computing facilities at Culham Science Centre.

References

[1] S.J. Zinkle, Phys. Plasma. 12 (2005) 058101.
[2] S.L. Dudarev, J. Nucl. Mater. 329–333 (2004) 1151.
[3] P. Ehrhart, P. Jung, H. Schultz, H. Ullmaier, Atomic Defects in Metals, Landolt-Bornstein New Series, vol. 25, Springer-Verlag, Berlin, 1991.
[4] H. Shultz, Mater. Sci. Eng. A 141 (1991) 149.
[5] M.S. Duesbury, V. Vitek, Acta Mater. 46 (1998) 1481.
[6] S. Tanaka, J. Fuss, H. Kugler, U. Dedek, H. Schultz, Radiat. Eff. 79 (1983) 87.
[7] S.D. Kenny, A. Horsfield, H. Fujitani, Phys. Rev. B 62 (2000) 4899;
K. Kohary, V. Burlakov, D.G. Pettifor, D. Nguyen-Manh, Phys. Rev. B 71 (2005) 184203.
[8] G. Kresse, J. Hafner, Phys. Rev. B 47 (1993) 558;
G. Kresse, J. Furthmuller, Phys. Rev. B 54 (1996) 11169.
[9] D. Nguyen-Manh, A.P. Horsfield, S.L. Dudarev, Phys. Rev. B 73 (2006) 020101, R.
[10] H. Johnson, G. Mills, K.W. Jacobsen, in: B.J. Berne, G. Ciccotti, D.F. Coker (Eds.), Classical and Quantum Dynamics in Condensed Phase Simulations, World Scientific, 1998, p. 385.
[11] P. Soderlind, L.H. Yang, J.A. Moriarty, Phys. Rev. B 61 (2000) 2579.
[12] F. Willaime, A. Satta, M. Nastar, O. Le Bacq, Int. J. Quant. Chem. 77 (2000) 927.
[13] T.R. Armstrong, H.A. Filius, A. van Veen, J.R. Heringa, J. Nucl. Mater. 203 (1993) 189.
[14] K. Yamakawa, H. Kugler, H. Schultz, Radiat. Eff. 105 (1988) 171.
[15] S. Han, L.A. Zepeda-Ruiz, G.J. Ackland, R. Car, D.J. Srolovitz, Phys. Rev. B 66 (2002) 220101.
[16] C. Domain, C.S. Becquart, Phys. Rev. B 65 (2002) 024103.
[17] C.C. Fu, F. Willaime, P. Ordejon, Phys. Rev. Lett. 92 (2004) 175503.
[18] G.Q. Liu, D. Nguyen-Manh, B.G. Liu, D.G. Pettifor, Phys. Rev. B 71 (2005) 174115.
[19] G.J. Ackland, R. Thetford, Philos. Mag. A 56 (1987) 15.
[20] P. Ehrhart, K.H. Robrock, H.R. Schober, in: R.A. Johnson, A.N. Orlov (Eds.), Physics of Radiation Effects in Crystals, Elsevier, Amsterdam, 1986.
[21] S.L. Dudarev, Philos. Mag 83 (2003) 3577.
[22] D. Nguyen-Manh, S.L. Dudarev, Mater. Sci. Eng. A 423 (2006) 74.